



Bacterial spore's fluorescence dependence on vaporised hydrogen peroxide concentration

Ott Rebane^{a,b*}, Marco Kirm^{a,c}, Larisa Poryvkina^b, Harri Hakkarainen^d and Sergey Babichenko^b

^a Institute of Physics, University of Tartu, W. Ostwald 1, 50411 Tartu, Estonia

^b LDI Innovation OÜ, Sära tee 7, 75312 Peetri, Estonia

^c Estonian Academy of Sciences, Kohtu 6, 10130 Tallinn, Estonia

^d Cleamix Oy, Lönnrotinkatu 2, 70500 Kuopio, Finland

Received 28 May 2021, accepted 6 August 2021, available online 15 March 2022

© 2022 Authors. This is an Open Access article distributed under the terms and conditions of the Creative Commons Attribution 4.0 International License CC BY 4.0 (<http://creativecommons.org/licenses/by/4.0>).

Abstract. Commonly used biological indicators for assessing the efficiency of decontamination procedures include the spores of *Bacillus atrophaeus* (BA) and *Geobacillus stearothermophilus* (GS). BA and GS spores emit tryptophan-like fluorescence around 320 nm when excited by 280 nm UV light. This fluorescence signal is highly dependent on vaporised hydrogen peroxide (VHP) concentration around the spores, since VHP quenches the fluorescence. In this study we investigated the precise influence of VHP concentration on the autofluorescence properties of BA and GS spores. For both types of spores, the fluorescence signal intensity was found to fall faster and to a relatively lower level when higher VHP concentration was applied. The shape of the signal fall-off as a function of time was found to be well approximated by biexponential decay functions with similar time-constants for BA and GS spores, finally resulting in the equilibrium (or plateau/residual) fluorescence intensity levels that were very different for these samples. The reasons for the fluorescence signal fall-off were investigated by spectral fluorescence signatures (SFS) of the spores. The SFS measurements of the spores during VHP decontamination revealed that the spectral maximum of tryptophan-like (Trp-like) fluorescence changes towards a smaller Stokes shift and has the intensity fall-off due to quenching and oxidation under VHP influence.

Keywords: vaporised hydrogen peroxide, *Geobacillus stearothermophilus*, *Bacillus atrophaeus*, decontamination, fluorescence.

INTRODUCTION

The Covid-19 pandemic has once again reminded humankind of how extensive damage can be caused even by relatively simple bio-pathogens if these are able to spread broadly. The spreading of pathogens can be significantly reduced by controlling social distancing, yet this has to be complemented by proper disinfection and decontamination efforts for greater influence. The necessity of bio-pathogen decontamination can be understood even more easily by mentioning examples such as multidrug-resistant bacteria on any hidden surface of a hospital room or infectious disease spread on surfaces of public transportation vehicles. Simply wiping every

surface in the contaminated room with a bleaching agent is often not possible. Furthermore, it is not even effective for certain materials, for example, porous surfaces or fabrics. Therefore, nowadays the more efficient and applicable decontamination efforts are handled by using gaseous media such as chlorine dioxide gas or vaporised hydrogen peroxide (VHP) [1]. An advantage of using gaseous decontamination media is its immediate contact with every surface of the room that is exposed to the air – no matter the spatial orientation or physical accessibility of the surfaces. Another advantage that is specific to hydrogen peroxide vapour, which is a subject of this study, stems from the fact that the leftover hydrogen peroxide decomposes into oxygen and water. In contrast to chlorine dioxide gas treatment, decomposition of VHP leaves no foul smell in the decontaminated rooms.

* Corresponding author, ott.rebane@ut.ee

Traditionally, the efficiency of a VHP decontamination procedure is monitored by placing biological indicators (BIs) such as the hard-to-kill spores of *Geobacillus stearothermophilus* (GS) or *Bacillus atrophaeus* (BA) in the room to be decontaminated, to the “hard-to-reach locations” where air flow might be partially or fully inhibited. These BIs at the hard-to-reach locations represent the worst case scenarios for the decontamination process. After decontamination has been carried out, the BIs are placed in an appropriate growth supporting medium to check their viability. If no growth is revealed after 1–7 days, then it can be finally concluded that the decontamination effort has indeed been successful. The delay of 1–7 days in the confirmation decision is definitely too long for many public rooms, therefore the authors have suggested using the dynamic change of the auto-fluorescence signal of the BIs as an additional indicator that can be exploited to evaluate the efficiency of the decontamination procedure in real time [2]. For a similar purpose of getting the quick feedback, VHP decontamination has been investigated by means of adenosine triphosphate bioluminescence assays [3], which offers a very different fluorescence approach to the methodology of this paper. Compared to the classical method, the dissimilar non-logarithmic signal behaviour revealed through the ATP assay approach makes it inappropriate for the decontamination monitoring. Admittedly, in the current paper the fluorescence fall-off of the tryptophan-like spectral region is not directly related to the cell death either as the quenching effect is much quicker than the oxidation effect. However, according to [4], the main oxidative damage causing cell death does not occur due to the DNA destruction, but due to the deterioration of nucleotides. Certainly, H_2O_2 does cause DNA damage in different modes [5], but according to [6], in the case of vaporised H_2O_2 the main damage is induced through its effect on key proteins and is very different from the effect of liquid H_2O_2 . Moreover, as stated in [7], the main spore killing mechanism is introduced by the damage of the spore inner membrane and is not even directly related to any DNA damage. Therefore, using a secondary effect to get a highly sensitive real-time indication about the decontamination progress is deemed to be justified.

Real-time monitoring of the VHP decontamination procedure by the autofluorescence fall-off effect of the pathogens is still of little use if not being quantified for each biological indicator at more than one VHP concentration. No presumptions can be made about the behaviour of different types of BIs influenced by VHP at various concentrations. Therefore, this effect needs to be systematically studied in order to explain all peculiarities of BI fluorescence quenching, which is the purpose of this paper.

MATERIALS AND METHODS

The biological indicators utilised in this study were the endospores of GS and BA bacteria. Both of these bacterial species are gram-positive with the thick cell walls and are known for their resilience against decontamination procedures [8]. Droplets of $\sim 10^8$ CFU (Colony Forming Unit)/mL liquid solutions were dried providing 10^6 CFU/cm² surface concentrations onto stainless steel plates, which were mounted inside the fluorometer during the VHP decontamination procedures. The fluorometer device employed for the measurements was the multichannel H2B-Spectral (LDI Innovation OÜ), which enables a real-time signal read-out at 340 nm/460 nm (nicotinamide adenine dinucleotide, NADH-like) and 280 nm/340 nm (Trp-like) spectral channels. The first shorter wavelength was used in excitation and the second in fluorescence detection. In this study, mainly the Trp-like spectral channel was applied.

Vaporised hydrogen peroxide was generated by a VCS-100 device (Cleamix Oy, see Fig. 1, top right), which establishes a pre-set VHP concentration in the room to be decontaminated with the help of a VHP concentration sensor, a VHP catalyser and a relevant PID controller. The VCS-100 device also monitors and controls the experimental conditions prohibiting condensation of VHP using the built-in hygrometer data and comparing it with the VHP concentration data. The condensation process (even to aerosol droplet) reduces contamination efficiency [9]. A large fan in the room was used to homogenise VHP concentration all over the room. In the case of GS spores, four different VHP concentrations were studied as a function of time (100 ppm, 200 ppm, 300 ppm and 400 ppm VHP, see Fig. 2 – vertical lines show the exact start and finish of each experiment) and in the case of BA spores, three different concentrations (100 ppm, 200 ppm, 300 ppm) were applied. In all cases, except for the 300 ppm exposure of BA, VHP concentration was first established and stabilised, and then the fluorometer with a spore sample was brought into the room. This procedure was needed for ensuring comparable conditions in such a way that the spores would immediately be affected by the pre-set VHP concentration and no differences in concentration ramp-up effects would influence the measurements. In our study, a small conference room was used to simulate the VHP decontamination procedure. It had a volume of 30 m³ and a sliding door enabling to quickly move the devices in and out without spoiling the VHP concentration. The temperature during the measurements varied from 21 to 25 °C and the relative humidity levels were between 50–80%. Simultaneously with the main measurements by a fluorometer, a series of SFS-GO spectrofluorometer (LDI Innovation OÜ) measurements were carried out, which enabled to cover a wider spectral range for studying the effect. This device is also less sensitive and provides much more destructive UV photons in the excitation.



Fig. 1. Top left – a side view of the rented conference room with a volume of 30 m³ in the unused office building, used in the experiments. Top right – a view inside the experimental room: the big box, in light blue colour, on the floor is the VHP catalyser, the black suitcase on the table is the VCS-100 VHP generation device with the VHP sensor hanging from the lid; the larger fan for air homogenisation is not visible in the picture. Bottom left – a top view of the H2B-Spectral fluorometer with a stainless steel sample disk inserted. Bottom right – a side view of the SFS-GO spectrofluorometer with the sample installed in the measurement handle on top of the device.

RESULTS

Each VHP exposure experiment with a real-time fluorometer read-out had a 20-minute duration and each GS experiment included the following samples: four dried droplets of spores and four wet droplets, which were later introduced into the suitable growth environment to check the viability of the spores after each experiment by means of the classical microbiology method. The comparison with the results of the classical method revealed that decontamination could be considered successful in most cases of the VHP concentration being above 100 ppm (see Table 1).

Geobacillus stearothermophilus spores

Spectral fluorescence signatures (SFS) were recorded for GS endospores as well as for live GS bacteria before and

after the VHP decontamination procedure (see Fig. 3 for details). The SFS spectra of GS spores in the tryptophan-like spectral region (here “Trp-like” has the following meaning: in addition to tryptophan 280 nm/348 nm, also the spectroscopic effects of phenylalanine 257 nm/282 nm and tyrosine 274 nm/303 nm amino acids can be detected in a close-by spectral region and summed into “tryptophan-like”) show a spectral shift towards shorter emission wavelengths (i.e. corresponding to a smaller Stokes shift) and a very sharp spectral intensity fall-off during the VHP decontamination. In contrast to the spores, in the case of GS bacteria, the spectral shift is not as obvious and the fluorescence intensity even increases after the completion of the VHP procedure. As specified in the discussion section, this increase is explained by denaturation of tyrosine-containing proteins.

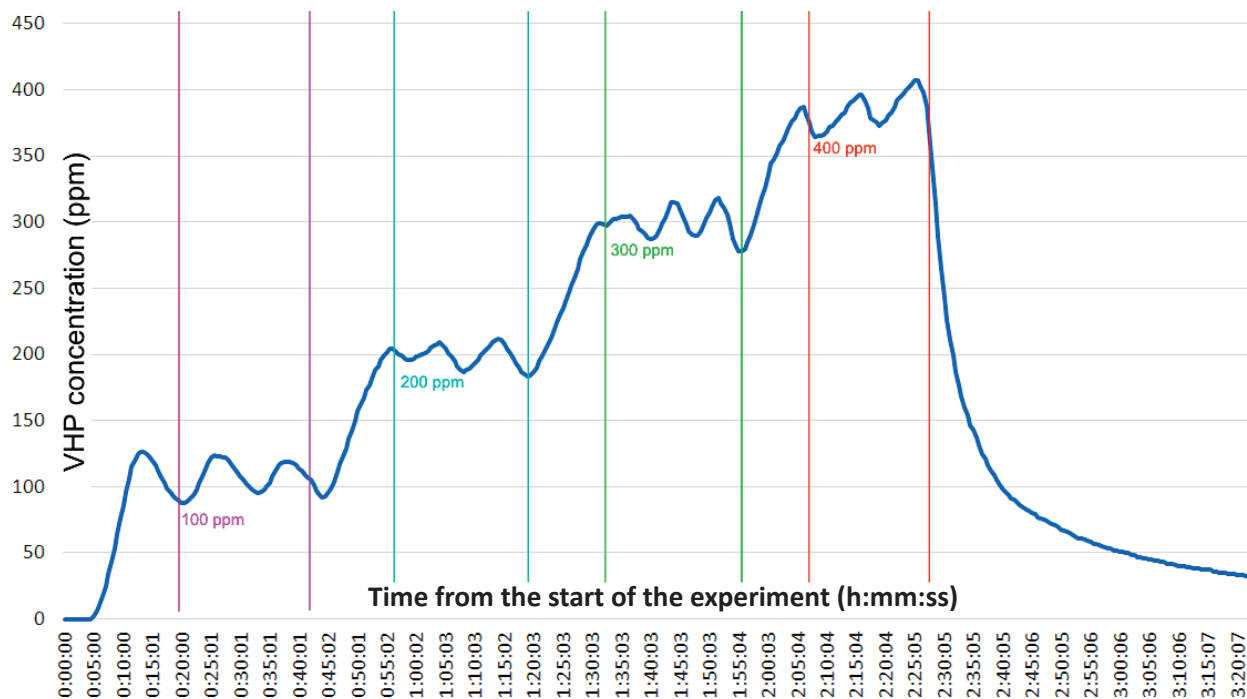


Fig. 2. VHP concentration as a function of time during GS spore decontamination experiments. Violet vertical bars show the beginning and end of exposure for 100 ppm, cyan for 200 ppm, green for 300 ppm and red for 400 ppm VHP concentrations, respectively.

Table 1. Results of the classical growth method for all GS experiments

#	Sample, H ₂ O ₂ concentration, exposure	CFU/sample
1	GS 10 μ L \times 4, 0 ppm, 20 min, dry (control)	10 000
2	GS 10 μ L \times 4, 0 ppm, 20 min, dry (control)	900
3	GS 50 μ L \times 4, 0 ppm, 20 min, wet (control)	636
4	GS 50 μ L \times 4, 0 ppm, 20 min, we (control)	900
5	GS 10 μ L \times 4, 100 ppm, 20 min, dry	182
6	GS 10 μ L \times 4, 100 ppm, 20 min, dry	700
7	GS 50 μ L \times 4, 100 ppm, 20 min, wet	<100
8	GS 50 μ L \times 4, 100 ppm, 20 min, wet	<100
9	GS 10 μ L \times 4, 200 ppm, 20 min, dry	<100
10	GS 10 μ L \times 4, 200 ppm, 20 min, dry	200
11	GS 50 μ L \times 4, 200 ppm, 20 min, wet	<100
12	GS 50 μ L \times 4, 200 ppm, 20 min, wet	<100
13	GS 10 μ L \times 4, 300 ppm, 20 min, dry	<100
14	GS 10 μ L \times 4, 300 ppm, 20 min, dry	<100
15	GS 50 μ L \times 4, 300 ppm, 20 min, wet	<100
16	GS 50 μ L \times 4, 300 ppm, 20 min, wet	<100
17	GS 10 μ L \times 4, 400 ppm, 20 min, dry	100
18	GS 10 μ L \times 4, 400 ppm, 20 min, dry	<100
19	GS 50 μ L \times 4, 400 ppm, 20 min, wet	<100
20	GS 50 μ L \times 4, 400 ppm, 20 min, wet	<100

Firstly, the intensity changes of the Trp-like spectral region were studied with a highly sensitive fluorometer H2B-Spectral under 280 nm excitation and at the 325–355 nm emission channel, selected by a bandpass filter at the multiple VHP concentrations. The fluorescence intensity

fall-off speed was detected to be dependent on VHP concentration – a higher VHP concentration caused a faster fall-off rate. Secondly, after sufficiently long VHP exposure it was discovered that the reached equilibrium (plateau) level, towards which the spectral intensity falls,

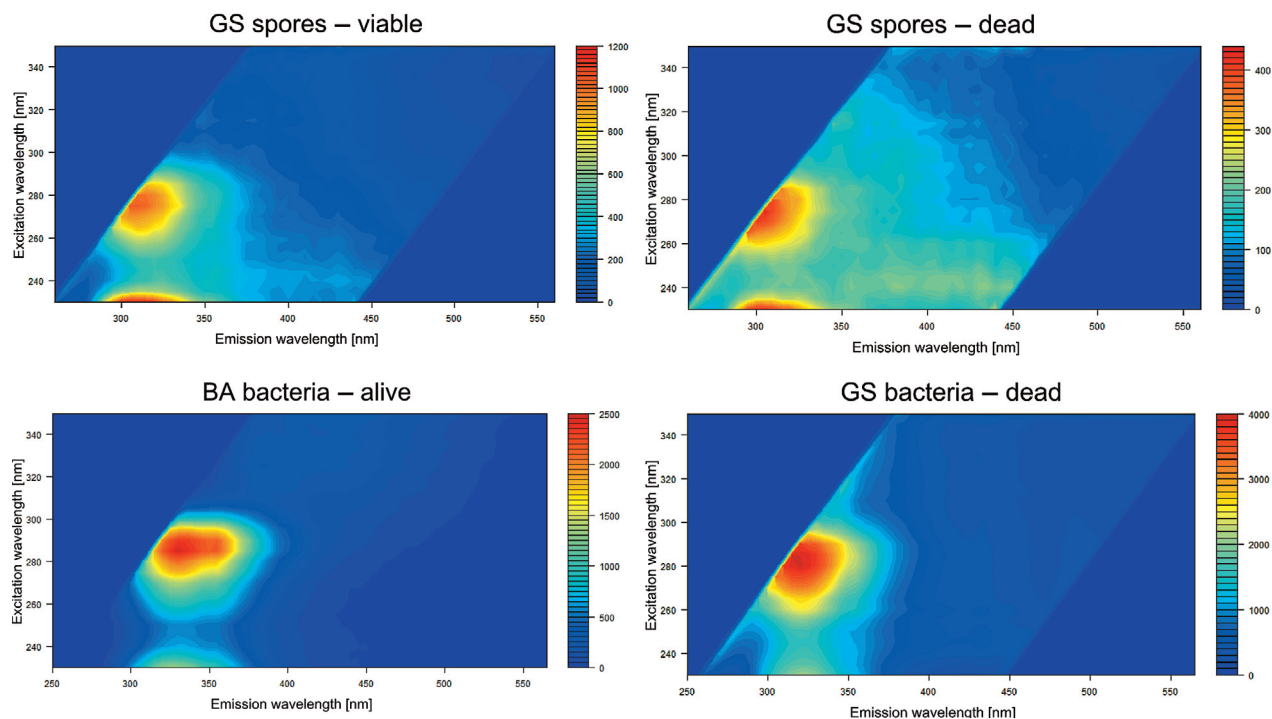


Fig. 3. SFS spectra of viable GS spores (top left), VHP-killed GS spores (top right), living GS bacteria (bottom left) and VHP-killed GS bacteria (bottom right). In SFS spectra, the vertical axis denotes the excitation wavelength, the horizontal axis shows the emission wavelength and the spectral intensity is colour-coded. The spectral maximum shifts towards shorter wavelengths in all decontamination experiments.

was also concentration-dependent. A higher VHP concentration led to lower relative fluorescence levels at the end of exposure, as can be expected due to fluorescence quenching effects and oxidation of hydrogen peroxide on tryptophan. Interestingly, the monoexponential fall-off suggested by the authors in [2] did not result in a sufficiently good mathematical fitting for most of the VHP concentrations, whereas a biexponential decay function led to an almost perfect fitting of experimental data for all concentrations. This, in turn, prompted the authors to seek a two-step physical damage mechanism as revealed by the mathematical analysis. As the second main finding besides the biexponential fall-off function, it was identified that the free member of the mathematical fitting functions (describing a plateau level of fluorescence) had a relatively simple mathematical relation to the VHP concentration. An exponential fitting function provided a good description between the VHP concentration and the relative fluorescence intensity recorded at least five minutes after the start of exposure (see right graph of Fig. 4 for details). While describing similar behaviour of the GS spores, the exponential function applied to the signal analysis showed significant differences at small VHP concentration variations (i.e. fluorescence is highly sensitive in the low-concentration region). Thus, the

monitoring of GS spore fluorescence is indeed suitable for following decontamination processes since the high VHP concentration values kill spores equally well in the timeframe of tens of minutes, while at the low VHP concentrations much longer time-scales are needed for achieving sufficient decontamination efficiencies, i.e. low VHP concentrations require more precise monitoring over time and the fall-off effect provides it.

Bacillus atrophaeus spores

The SFS spectra were also measured for the BA spores and bacteria before and after the VHP decontamination procedure (see Fig. 5). In both cases, also the Trp-like spectral peak (280 nm/330 nm) was observed to shift towards shorter emission wavelengths. As regards BA endospores, the intensity of the main fluorescence maximum was reduced by the procedure, while in the case of bacteria this did not occur and even an increase in the signal intensity was detected. Other spectral regions showed a much smaller change during the VHP decontamination procedure as well.

With reference to BA spores, the fluorometer measurement protocol was not fully established (the sample insertion was performed too early and higher VHP concentrations were not yet achieved). Therefore, only

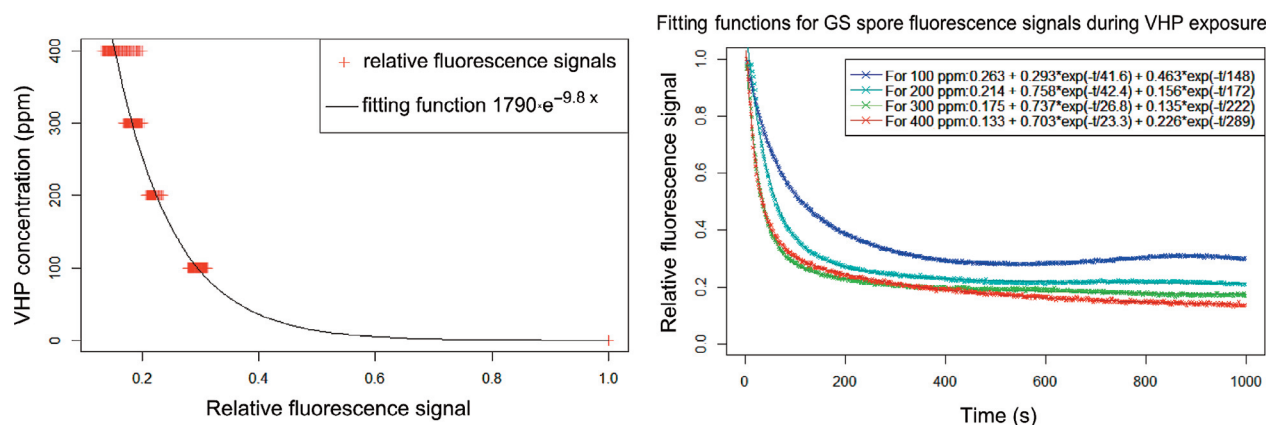


Fig. 4. Left graph – VHP concentration values plotted as a function of the relative fluorescence intensity levels (compared to the initial fluorescence level) that were recorded after >5 minutes from the beginning of VHP exposure. The single exponential fitting seems to describe really well the GS spores during the VHP decontamination process. Right graph – intensity of relative fluorescence levels in the Trp-like spectral region as a function of time at 100 ppm, 200 ppm, 300 ppm and 400 ppm VHP concentrations. Data was measured in real time after placing the samples ($t = 0$) in the experimental room where VHP decontamination was carried out. The values of biexponential fitting functions are also shown in the legend of the graph and in Table 2.

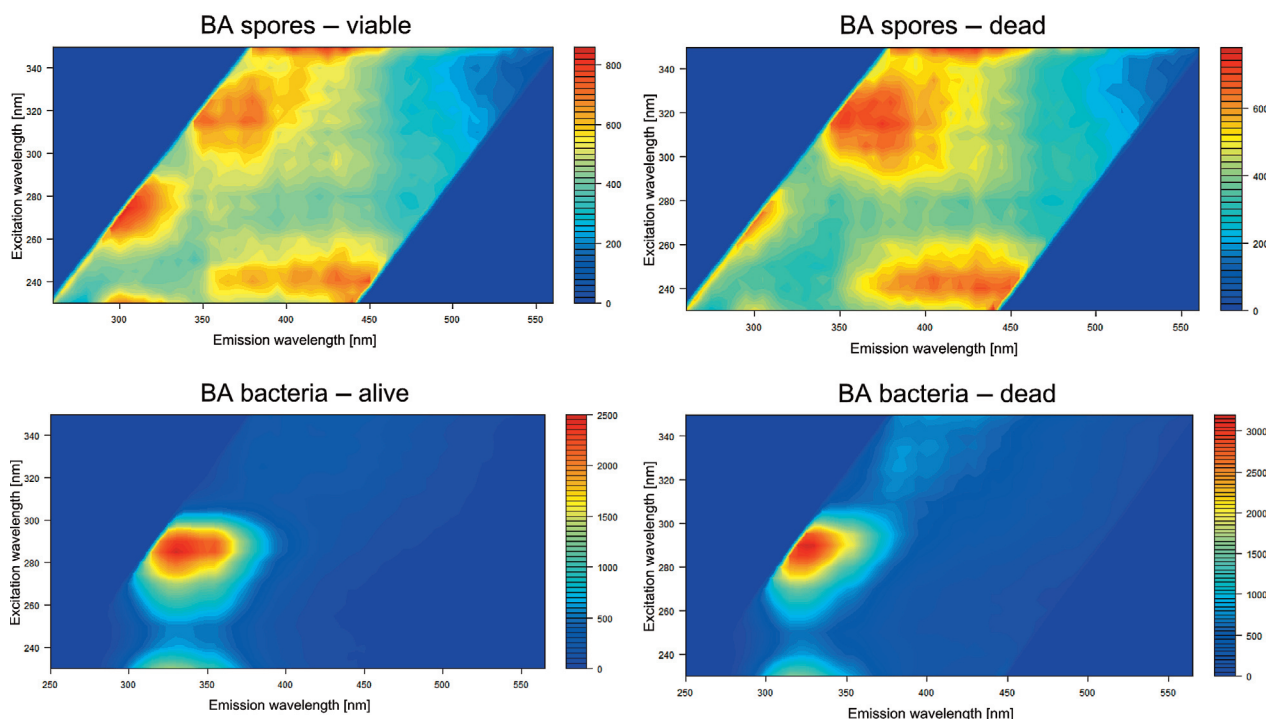


Fig. 5. SFS spectra of viable BA spores (top left), VHP-killed BA spores (top right), living BA bacteria (bottom left) and VHP-killed BA bacteria (bottom right). In SFS spectra, the vertical axis marks the excitation wavelength, the horizontal axis shows the emission wavelength and the spectral intensity is colour-coded.

two concentrations could be directly compared with the GS spore results – 100 ppm and 200 ppm instantaneous measurements. In the case of BA spores, using the biexponential function resulted in an almost perfect fitting

to experimental data, but signal intensity in the plateau region was at much higher levels compared to GS spores. Also, the analysis of the relative signal as a function of VHP concentration did not give such a well-defined

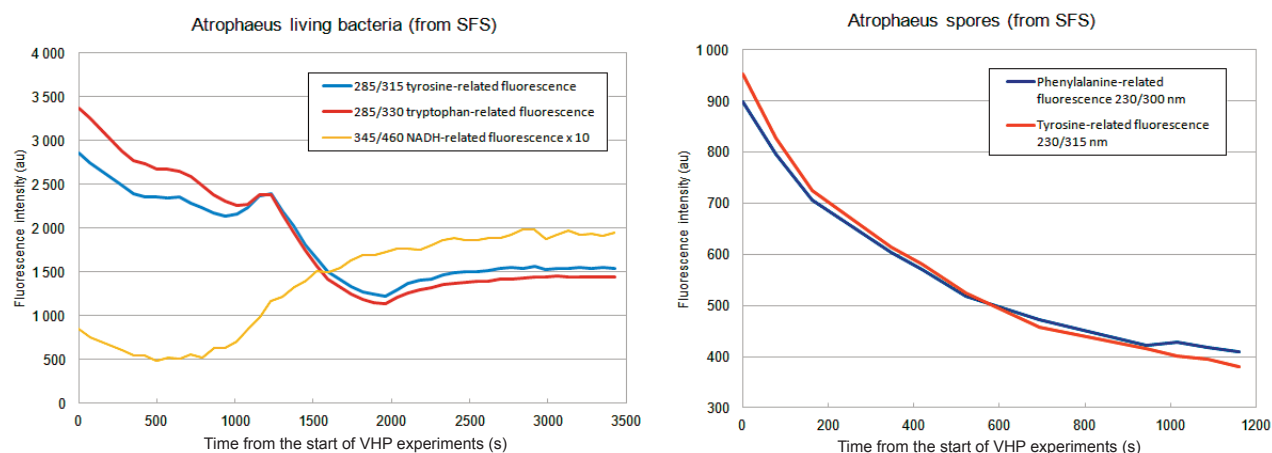


Fig. 6. Left graph – comparison of intensities of tryptophan fluorescence (red line) and more tyrosine-like fluorescence (blue line) as a function of time during VHP exposure (in seconds). The yellow line represents the 345 nm/460 nm signal that is associated with the “NADH-like” fluorescence region, much of which can be attributed to oxidation induced fluorescence [10,11]. The VHP concentration was ~ 500 ppm. A clear activity similar to conformational change is revealed at ~ 1250 seconds, where one can assume that denaturation of important proteins is taking place. Right graph – in the spores of the same bacteria, one can see the longer-wavelength tyrosine-tryptophan peak's emission also fall at a faster rate compared to phenylalanine-tyrosine, indicating similar energy-transfer disruption processes during the VHP process.

exponential fitting function, rather leaving much room for interpretation.

To get a clearer understanding of the possible causes of the (biexponential) fall-off of the measured tryptophan-like signal, the full SFS spectra with 5 nm resolution were measured in real time also for the BA bacteria. We performed such measurements at the wavelengths with typical maxima for the tryptophan region (recorded at 285 nm/330 nm) as well as for the tyrosine region (recorded at 285 nm/315 nm) of the spectra. One can see a distinct difference in the signal behaviour during the VHP decontamination procedure. The tryptophan-related signal (red line in Fig. 6) falls much more abruptly compared to the tyrosine-related fluorescence signal (blue line).

In the case of BA spores' (Fig. 6, right graph) SFS data, a similar effect can be seen – the longer-wavelength fluorescence component (red line) is seen to fall off at a faster rate compared to the shorter-wavelength signal. Due to the elastic scattering (reflection) peak of excitation covering some of the 285 nm/300 nm signal, it is assumed here that the emission signal is more or less independent of the excitation wavelength, and the 230 nm/300 nm and 230 nm/315 nm peaks are plotted. The shorter-wavelength intensity line (blue) can tentatively be assigned to phenylalanine, while the longer-wavelength graph is more associated with tyrosine. VHP influence may disrupt energy transfer between these amino acids, causing therefore fewer energy transfers from phenylalanine to tyrosine and from tyrosine to tryptophan, having the joint effect of shifting the fluorescence maximum to shorter wavelengths.

DISCUSSION

Bacterial endospores are known to be highly resistant to many decontamination procedures, not only because their DNA is cushioned between large amounts ($\sim 10\%$ of spore content) of dipicolinic acid, but also because the endospores have at least four layers of coat [12]. The three outer layers prevent large unwanted molecules from entering the spore, while the inner layer blocks smaller molecules such as hydrogen peroxide used in the decontamination process. The inner layer is also the one that the spore uses to rebuild the bacterial coat after germination. According to [13], treatment with oxidising agents damages the inner membrane and sensitises the spores to any subsequent stress. Thus, it is the oxidative or conformational change induced destruction of some parts of this spore's inner layer that prevents germination of bacterial endospores after exposing them to hydrogen peroxide gas. Cortezzo et al. [13] also established the hypothesis that oxidative damage to the key proteins of the spore's inner membrane may be the main cause of damage. The damaged spores may not germinate and even if they do, the inner membrane is so badly damaged that the spores die rapidly.

The fact that most of the tryptophan is actually bound in the inner coat of the spore is another piece of important information for the discussion about the fluorescence fall-off process, as reported by [14]. The exact protein composition of the various cell wall layers as well as the inner parts is not easily detectable. However, according to

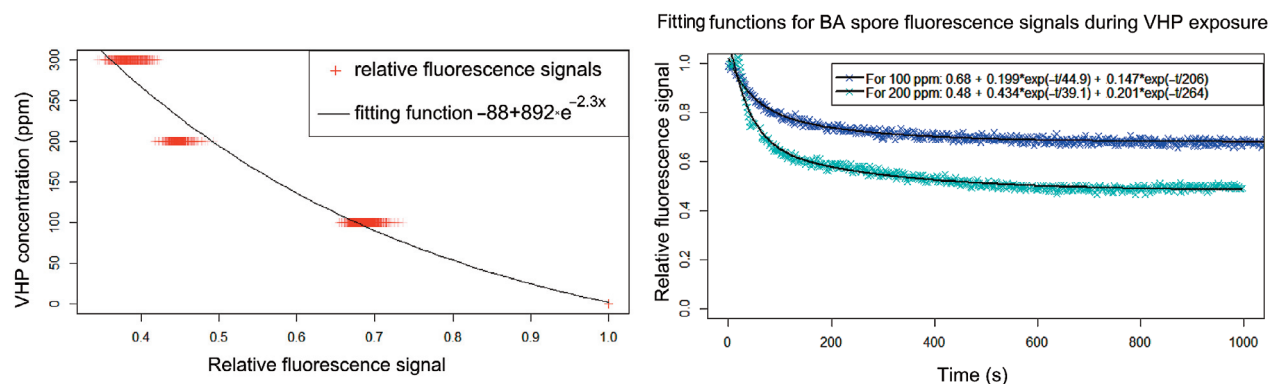


Fig. 7. Left graph – BA spore’s relative fluorescence signal intensity plotted as a function of VHP concentration. Right graph – relative fluorescence signal intensity as a function of time at 100 ppm (blue) and 200 ppm (cyan) VHP concentrations. The values of the biexponential fitting are shown in the top-right corner.

[15–17], they have much more tyrosine, another well-fluorescing amino acid, than the outer spore coat.

Tyrosine is typically much more abundant than tryptophan. As stated in [18], tyrosine fluorescence emission actually increases when proteins unfold. This provides a rather consistent explanation for the signal increase in the case of GS and BA bacteria after VHP exposure (see the after-VHP-exposure intensities in Fig. 6 of [2]). After intense VHP exposure the proteins containing tyrosine become unfolded and thus have a higher fluorescence signal. Moreover, tyrosine is then more decoupled from any close-by tryptophan residue so that energy transfer to tryptophan will not occur and the average emission wavelength will shift towards shorter wavelengths where the tyrosine emission spectrum is located.

During the VHP decontamination procedure, the biexponential function of fluorescence quenching with a characteristic time in minutes was revealed in the experiments. This could be resulted from slow diffusion of H_2O_2 into the proteins of microorganisms and quenching of the fluorescence of accessible residues of tryptophan and tyrosine. The biexponential fitting function could be explained by a different effect of VHP on tryptophan and tyrosine during VHP exposure providing different time constants.

It can be seen in the SFS spectra of bacteria and spores that the fluorescence maximum is shifted towards shorter-

wavelength emission during VHP exposure. Typically, an efficient energy transfer process from tyrosine to tryptophan is taking place [19], but H_2O_2 denaturing/unfolding of the normal protein structure disrupts the energy transfer. This causes the shift of the fluorescence maximum towards shorter wavelengths.

In the SFS of spores the fluorescence maximum is located at shorter wavelengths (ex/em = 275/315 nm) compared with the tryptophan fluorescence maximum of bacteria (ex/em = 285/330 nm). This coincides with the fact that external coats of spores contain mainly tyrosine. Under VHP exposure the tyrosine spectra are still shifted to shorter wavelengths, similar to the blue-shift for bacteria. This allows us to suppose that VHP breaks the energy transfer between phenylalanine and tyrosine [20], caused by the conformational changes in proteins located in the external coats of the spores. Taking into account the rather low quantum yield of phenylalanine fluorescence, it is possible to conclude that quenching is observed consistently from the external accessible coats of spores down to buried tyrosine.

In general, during VHP exposure four effects may cause reduction in the fluorescence [21]: protein decoupling processes, direct quenching, solvatochromic shift, lower and re-shifted fluorescence in denatured proteins. In the biexponential curve the faster component (25–45 s, see Table 2

Table 2. Biexponential fitting parameters for Trp-like fluorescence peak intensity change during HPV decontamination of BA and GS spores

$A+B\cdot\exp(-t/C)+D\cdot\exp(-t/E)$	A	B	C	D	E
BA spores 100 ppm	0.68	0.199	44.9	0.147	206
BA spores 200 ppm	0.48	0.434	39.1	0.201	264
GS spores 100 ppm	0.263	0.294	41.6	0.463	148
GS spores 200 ppm	0.214	0.758	42.4	0.156	172
GS spores 300 ppm	0.175	0.737	26.8	0.135	222
GS spores 400 ppm	0.133	0.703	23.3	0.226	289

Column C) could be related to the accessible tyrosine located in the external coats, while the slower component (150–250 s, see Table 2 Column E) is tentatively attributed to the tyrosine fluorescence mostly buried in the inner parts.

The end of the quenching process manifested by the plateau in the dynamic fluorescence curves in Figs 4 and 7 indicates that denaturation of protein has taken place, and the molecular structure remains unchanged from that time onwards.

Figure 6 points to the important differences in tyrosine-like fluorescence compared to tryptophan-like fluorescence. This circumstance supports the hypothesis that the peculiarities of the fluorescence signal change can probably be attributed to VHP interaction with tryptophan and tyrosine during the denaturation process.

CONCLUSIONS

This is the first time the mathematical relations backed with a model of the underlying processes have been established between BI (GS and BA spores) fluorescence intensity and the VHP decontamination agent concentration, well described by a set of exponential functions.

The biexponential fluorescence quenching function can be explained by the model where quenching of accessible tyrosine in spore proteins located in the external coats is the reason for the fast component revealed, as there are multiple effects that reduce tyrosine fluorescence intensity. The quenching of buried tyrosine fluorescence in spore proteins may be responsible for the slower quenched component. The spectral fluorescence signatures, recorded in real-time mode during VHP decontamination, support the hypothesis that the peculiarities of fluorescence patterns in SFS during VHP treatment are related to the denaturation processes of cell protein.

The dynamics of protein fluorescence quenching caused by VHP treatment as well as the spectral changes of the characteristic spectral patterns of SFS can be used as the indicators of VHP efficiency for the optimisation of the decontamination treatment.

ACKNOWLEDGEMENTS

This research was supported by funding from the Finnish Government Development Grants through Cleamix Oy, the ERDF funding in Estonia granted to the Centre of Excellence TK141 “Advanced materials and high-technology devices for sustainable energetics, sensorics and nanoelectronics” (project No. 2014-2020.4.01.15-0011) and the Estonian Research Council grant PRG-629. O. Rebane acknowledges the support by the Graduate School of Functional Materials and Technologies for receiving

funding from the European Regional Development Fund at the University of Tartu, Estonia. The authors would like to extend their gratitude to the VTT Technical Research Centre of Finland and Xhome Oy. The publication costs of this article were partially covered by the Estonian Academy of Sciences.

REFERENCES

1. Otter, J. A., Yezli, S., Barbut, F. and Perl, T. M. An overview of automated room disinfection systems: When to use them and how to choose them. In *Decontamination in Hospitals and Healthcare* (Walker, J., ed.). Second edition. Woodhead Publishing, 2020, 323–369. <https://doi.org/10.1016/B978-0-08-102565-9.00015-7>
2. Rebane, O., Hakkarainen, H., Kirm, M., Poryvkina, L., Sobolev, I., Wilska, P. and Babichenko, S. Real-time monitoring of hydrogen peroxide vapour decontamination of bacterial spores by means of UV fluorimetry. *Proc. Estonian Acad. Sci.*, 2021, **70**(1), 51–61. <https://doi.org/10.3176/proc.2021.1.06>
3. Colbert, E. M., Gibbs, S. G., Schmid, K. K., High, R., Lowe, J. J., Chaika, O. and Smith, P. W. Evaluation of adenosine triphosphate (ATP) bioluminescence assay to confirm surface disinfection of biological indicators with vaporised hydrogen peroxide (VHP). *Healthcare Infect.*, 2015, **20**(1), 16–22. <https://doi.org/10.1071/HI14022>
4. Hirakawa, K. Biomolecules oxidation by hydrogen peroxide and singlet oxygen. In *Reactive Oxygen Species (ROS) in Living Cells* (Filip, C. and Albu, E., eds). IntechOpen, 2017. <https://doi.org/10.5772/intechopen.71465>
5. Linley, E., Denyer, S. P., McDonnell, G., Simons, C. and Maillard, J.-Y. Use of hydrogen peroxide as a biocide: new consideration of its mechanisms of biocidal action. *J. Antimicrob. Chemother.*, 2012, **67**(7), 1589–1596. <https://doi.org/10.1093/jac/dks129>
6. Finnegan, M., Linley, E., Denyer, S. P., McDonnell, G., Simons, C. and Maillard, J.-Y. Mode of action of hydrogen peroxide and other oxidizing agents: differences between liquid and gas forms. *J. Antimicrob. Chemother.*, 2010, **65**(10), 2108–2115. <https://doi.org/10.1093/jac/dkq308>
7. Wood, J. P. and Adrion, A. C. Review of decontamination techniques for the inactivation of *Bacillus anthracis* and other spore-forming bacteria associated with building or outdoor materials. *Environ. Sci. Technol.*, 2019, **53**(8), 4045–4062. <https://doi.org/10.1021/acs.est.8b05274>
8. Luftman, H. S. and Regits, M. A. *B. atrophaeus* and *G. stearothermophilus* biological indicators for chlorine dioxide gas decontamination. *Appl. Biosaf.*, 2008, **13**(3), 143–157. <https://doi.org/10.1177%2F153567600801300304>
9. Holmdahl, T., Lanbeck, P., Wullt, M. and Walder, M. H. A head-to-head comparison of hydrogen peroxide vapor and aerosol room decontamination systems. *Infect. Control Hosp. Epidemiol.*, 2011, **32**(9), 831–836. <https://doi.org/10.1086/661104>
10. Tikhonova, T. N., Rovnyagina, N. R., Zhrebker, A. Y., Sluchanko, N. N., Rubekina, A. A., Orekhov, A. S. et al. Dissection of the deep-blue autofluorescence changes

- accompanying amyloid fibrillation. *Arch. Biochem. Biophys.*, 2018, **651**, 13–20. <https://doi.org/10.1016/j.abb.2018.05.019>
11. Semenov, A. N., Yakimov, B. P., Rubekina, A. A., Gorin, D. A., Drachev, V. P., Zarubin, M. P. et al. The oxidation-induced autofluorescence hypothesis: red edge excitation and implications for metabolic imaging. *Molecules*, 2020, **25**(8), 1863. <https://doi.org/10.3390/molecules25081863>
 12. McKenney, P., Driks, A. and Eichenberger, P. The *Bacillus subtilis* endospore: assembly and functions of the multi-layered coat. *Nat. Rev. Microbiol.*, 2013, **11**(1), 33–44. <https://doi.org/10.1038/nrmicro2921>
 13. Cortezzo, D. E., Koziol-Dube, K., Setlow, B. and Setlow, P. Treatment with oxidizing agents damages the inner membrane of spores of *Bacillus subtilis* and sensitizes spores to subsequent stress. *J. Appl. Microbiol.*, 2004, **97**(4), 838–852. <https://doi.org/10.1111/j.1365-2672.2004.02370.x>
 14. Li, R., Dhankhar, D., Chen, J., Cesario, T. C. and Rentzepis, P. M. A tryptophan synchronous and normal fluorescence study on bacteria inactivation mechanism. *Proc. Natl. Acad. Sci. U. S. A.*, 2019, **116**(38), 18822–18826. <https://doi.org/10.1073/pnas.1909722116>
 15. Munoz, L., Sadaie, Y. and Doi, R. H. Spore coat protein of *Bacillus subtilis*. Structure and precursor synthesis. *J. Biol. Chem.*, 1978, **253**(19), 6694–6701. <https://pubmed.ncbi.nlm.nih.gov/99446/>
 16. Goldman, R. C. and Tipper, D. J. *Bacillus subtilis* spore coats: complexity and purification of a unique polypeptide component. *J. Bacteriol.*, 1978, **135**(3), 1091–1106. <https://jb.asm.org/content/135/3/1091>
 17. Bhattacharyya, P. and Bose, S. K. Amino acid composition of cell wall and spore coat of *Bacillus subtilis* in relation to mycobactin production. *J. Bacteriol.*, 1967, **94**(6), 2079–2080. <https://jb.asm.org/content/94/6/2079>
 18. Zhdanova, N. G., Shirshin, E. A., Maksimov, E. G., Panchishin, I. M., Saletsky, A. M. and Fadeev, V. V. Tyrosine fluorescence probing of the surfactant-induced conformational changes of albumin. *Photochem. Photobiol. Sci.*, 2015, **14**(5), 897–908. <http://dx.doi.org/10.1039/C4PP00432A>
 19. Ghisaidoobe, A. B. T. and Chung, S. J. Intrinsic tryptophan fluorescence in the detection and analysis of proteins: A focus on Förster resonance energy transfer techniques. *Int. J. Mol. Sci.*, 2014, **15**(12), 22518–22538. <https://dx.doi.org/10.3390%2Fijms151222518>
 20. Lakowicz, J. R. *Principles of Fluorescence Spectroscopy*. 3rd edition. Springer, Boston, MA, 2006. <https://link.springer.com/book/10.1007/978-0-387-46312-4>
 21. Vivian, J. T. and Callis, P. R. Mechanisms of tryptophan fluorescence shifts in proteins. *Biophys. J.*, 2001, **80**(5), 2093–2109. [https://doi.org/10.1016/S0006-3495\(01\)76183-8](https://doi.org/10.1016/S0006-3495(01)76183-8)

Bakterisporide fluorestsentsi sõltuvus ümbritsevast vesinikperoksiidgaasi kontsentratsioonist

Ott Rebane, Marco Kirm, Larisa Poryvkina, Harri Hakkarainen ja Sergey Babichenko

Tavaliselt kasutatakse vesinikperoksiidgaasiga läbiviidava puhastusprotseduuri efektiivsuse hindamiseks *Bacillus atrophaeus* (BA) ja *Geobacillus stearothermophilus* (GS) bakterite spore. BA ja GS spoorid fluorestseeruvad trüptofaanile sarnase spektriga 320 nm juures, kui neid ergastada 280 nm UV footonitega. Taolise fluorestsents-signaali intensiivsus on tugevasti sõltuv vesinikperoksiidgaasi kontsentratsioonist spooride ümbruses, sest vesinikperoksiid kustutab nende fluorestsentsi. Käesolevas uurimuses oleme vaadelnud vesinikperoksiidgaasi erinevate kontsentratsioonide täpsemat mõju BA ja GS spooride autofluorestsentsile. Mõlemat tüüpi spooride korral leiti, et fluorestsentsi intensiivsus kustub kiiremini ja madalamale lõpptasemele, kui vesinikperoksiidi kontsentratsioon oli kõrgem. Fluorestsentsi intensiivsuse vähenemise ajasõltuvus lähendub hästi kahe-eksponentsiaalse kustumisfunktsiooniga, mille ajakonstandid BA ja GS spooride jaoks olid sarnased, kuid fluorestsentsi lõpptasemed üpris erinevad protsessi lõpus. Fluorestsents-signaali tugevuse langemise põhjuseid uuriti Spektraalsete Fluorestsentsi Sõrmejälgede (SFS) analüüsi abil. Spooride SFS spektrite mõõtmised vesinikperoksiidgaasi puhastusprotseduuri ajal näitasid, et kiirgusspektrite maksimumid nihkusid lühemate lainepikkuste suunas ning ühtlasi fluorestsentsi intensiivsus vähenes vesinikperoksiidi mõjul.